gels

MDPI

*Article*

# Alleviating Effect of a Magnetite ($Fe_3O_4$) Nanogel against Waterborne-Lead-Induced Physiological Disturbances, Histopathological Changes, and Lead Bioaccumulation in African Catfish

**Afaf N. Abdel Rahman [1,*], Basma Ahmed Elkhadrawy [2], Abdallah Tageldein Mansour [3,4,*], Heba M. Abdel-Ghany [5], Engy Mohamed Mohamed Yassin [6], Asmaa Elsayyad [7], Khairiah Mubarak Alwutayd [8], Sameh H. Ismail [9] and Heba H. Mahboub [1,*]**

1 Department of Aquatic Animal Medicine, Faculty of Veterinary Medicine, Zagazig University, Zagazig 44519, Egypt
2 Department of Forensic Medicine and Toxicology, Faculty of Veterinary Medicine, University of Sadat City, Sadat City 32897, Egypt; basma.elkhadrawy@vet.usc.edu.eg
3 Animal and Fish Production Department, College of Agricultural and Food Sciences, King Faisal University, P.O. Box 420, Hofuf 31982, Saudi Arabia
4 Fish and Animal Production Department, Faculty of Agriculture (Saba Basha), Alexandria University, Alexandria 21531, Egypt
5 Department of Pathology, Faculty of Veterinary Medicine, Zagazig University, Zagazig 44519, Egypt; heba.vet@yahoo.com
6 Department of Biochemistry, Faculty of Veterinary Medicine, Zagazig University, Zagazig 44519, Egypt; drengyyassin7@gmail.com
7 Department of Pharmacology, Faculty of Veterinary Medicine, Mansoura University, Mansoura 35516, Egypt; asmaa_ezat@mans.edu.eg
8 Department of Biology, College of Science, Princess Nourah bint Abdulrahman University, P.O. Box 84428, Riyadh 11671, Saudi Arabia; kmalwateed@pnu.edu.sa
9 Faculty of Nanotechnology for Postgraduate Studies, Cairo University, Sheikh Zayed Branch Campus, Giza 12588, Egypt; drsameheltayer@yahoo.com
* Correspondence: afne56@gmail.com (A.N.A.R.); amansour@kfu.edu.sa (A.T.M.); hhhmb@yahoo.com (H.H.M.)

**Abstract:** Heavy metal toxicity is an important issue owing to its harmful influence on fish. Hence, this study is a pioneer attempt to verify the in vitro and in vivo efficacy of a magnetite ($Fe_3O_4$) nanogel (MNG) in mitigating waterborne lead (Pb) toxicity in African catfish. Fish ($n$ = 160) were assigned into four groups for 45 days. The first (control) and second (MNG) groups were exposed to 0 and 1.2 mg $L^{-1}$ of MNG in water. The third (Pb) and fourth (MNG + Pb) groups were exposed to 0 and 1.2 mg $L^{-1}$ of MNG in water and 69.30 mg $L^{-1}$ of Pb. In vitro, the MNG caused a dramatic drop in the Pb level within 120 h. The Pb-exposed group showed the lowest survival (57.5%) among the groups, with substantial elevations in hepato-renal function and lipid peroxide (MDA). Moreover, Pb exposure caused a remarkable decline in the protein-immune parameters and hepatic antioxidants, along with higher Pb residual deposition in muscles and obvious histopathological changes in the liver and kidney. Interestingly, adding aqueous MNG to Pb-exposed fish relieved these alterations and increased survivability. Thus, MNG is a novel antitoxic agent against Pb toxicity to maintain the health of *C. gariepinus*.

**Keywords:** *Clarias gariepinus*; health status; lead toxicity; magnetite nanogel; nanotechnology; tissue architecture

check for updates

**Citation:** Rahman, A.N.A.; Elkhadrawy, B.A.; Mansour, A.T.; Abdel-Ghany, H.M.; Yassin, E.M.M.; Elsayyad, A.; Alwutayd, K.M.; Ismail, S.H.; Mahboub, H.H. Alleviating Effect of a Magnetite ($Fe_3O_4$) Nanogel against Waterborne-Lead-Induced Physiological Disturbances, Histopathological Changes, and Lead Bioaccumulation in African Catfish. *Gels* **2023**, *9*, 641. https://doi.org/10.3390/gels9080641

Academic Editors: Daxin Liang, Ting Dong, Yudong Li and Caichao Wan

Received: 7 July 2023
Revised: 2 August 2023
Accepted: 3 August 2023
Published: 8 August 2023

**Copyright:** © 2023 by the authors. Licensee MDPI, Basel, Switzerland. This article is an open access article distributed under the terms and conditions of the Creative Commons Attribution (CC BY) license (https://creativecommons.org/licenses/by/4.0/).

## 1. Introduction

With the introduction of harmful compounds into the aquatic environment, public health issues connected to environmental pollution are receiving much attention. Heavy

metal (HM) pollution is considered one of the most disastrous problems threatening aquatic and human life [1]. Fish are considered a pivotal indicator of aquatic environments for the assessment of the severity of HM toxicity, which constitutes a major hazard for all fish consumers [2,3].

African catfish (*Clarias gariepinus*) has been used to assess HM toxicity. The recent literature reveals the susceptibility of *C. gariepinus* to various HMs and verifies the deleterious impacts of HMs by inducing behavioral changes, immune–antioxidant impairments, and bioaccumulation [4–6]. Lead (Pb) is among the most hazardous HMs and is toxic even in low amounts for aquatic animals and humans, resulting in toxic impacts and accelerating different diseases [7]. In aquaculture, exposure to Pb induces oxidative stress, bioaccumulation, neurotoxicity, and immune dysfunction [8]. In *C. gariepinus* and Nile tilapia (*Oreochromis niloticus*), Pb toxicity causes several issues, including hepato-renal toxicity, oxidative damage, histopathological changes, and higher mortality rates [9,10].

Currently, the application of nanomaterials has been proven to have great success in drug delivery, antimicrobial uses, and remediating toxicity caused by either chemical toxicants or HMs in freshwater fishes [11–14]. Regarding the removal of HMs, engineered nanomaterials represent novel and successful approaches compared to traditional methods. Among the recently formulated nanoparticles, magnetite ($Fe_3O_4$) nanoparticles have interesting electric and magnetic properties and unlimited physical and chemical characteristics at the nanoscale [15,16]. The nano-magnetite form of iron has wide applications in the industry (magnetic recording media, soft magnetic materials, and coloring) and medical sectors (drug delivery, in vivo therapeutic technology, cell separation, and imaging) [17,18]. The magnetite nanocomposites prepared by the sol–gel method have several advantages, including low-cost preparation, toxicity-free iron salts, small particle size, and good dispersion in the solvent [16]. Magnetite nanoparticles ($Fe_3O_4$) succeeded in removing 66% of copper from a solution after 15 min [19]. Magnetite nanoparticles ($Fe_3O_4$ NPs) have been used in *O. niloticus* to chelate mercury (Hg) in vitro, in addition to boosting the immune–antioxidant status and liver and kidney function in vivo [14]. Nanogels (NGs) refer to small, aqueous, swollen nanoparticles composed of nano-scaled polymeric chains [20]. Recently, NGs have emerged as very promising and flexible biomaterials utilized in several applications, such as catalysts, sensing materials, or environmental adsorbents. Their characteristics (such as their wide surface area, flexibility in size, ability to carry molecules, and encapsulation of a high percentage of water when suspended in the fluid) enable their use for drug delivery [21,22]. NGs have been reported in novel environmental fields to eliminate organic toxicants and agrochemicals [23,24]. These contaminants can be trapped inside the NGs, and then removed from the environment [25,26]. In addition, a magnetic nanocomposite sol–gel of iron oxide nanoparticles coated with titanium dioxide efficiently removed aluminum and iron ions from contaminated water [27].

Therefore, this novel study is carried out to investigate the potent magnetic power of a magnetite nanogel (MNG) to mitigate the waterborne toxicity induced by Pb ions via testing their adsorption capacity and, accordingly, testing their magnetic effect to prevent Pb bioaccumulation in muscles. In addition, this study provides an assessment of the promising role of MNG on the protein profile, hepato-renal function, immune responses, tissue antioxidants, and the histological picture of African catfish.

## 2. Results

### 2.1. MNG Characterization

Figures 1–3 display various types of MNG characterization findings. X-ray diffraction (XRD) analysis demonstrated the fingerprint curve and data for magnetite according to the Brucker Database library, which conformed to validate our synthesis method without any secondary phases (Figure 1A). Dynamic light scattering (DLS) and zeta potential data showed a homogenous size (one peak) of 60 nm (Figure 1B). Due to a substantial degree of zeta potential (−35 mV), the results demonstrated a superior colloidal structure in aqueous solution (Figure 1C).

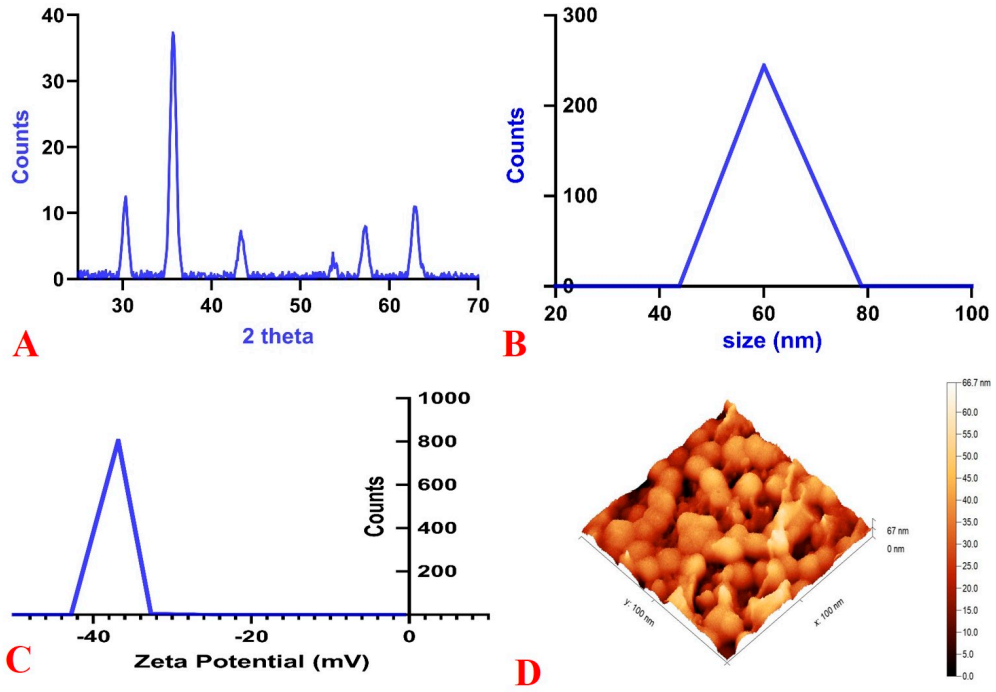


**Figure 1.** Characterization patterns of magnetite nanogel: (**A**) XRD, (**B**) DLS, (**C**) Zeta potential, and (**D**) AFM.

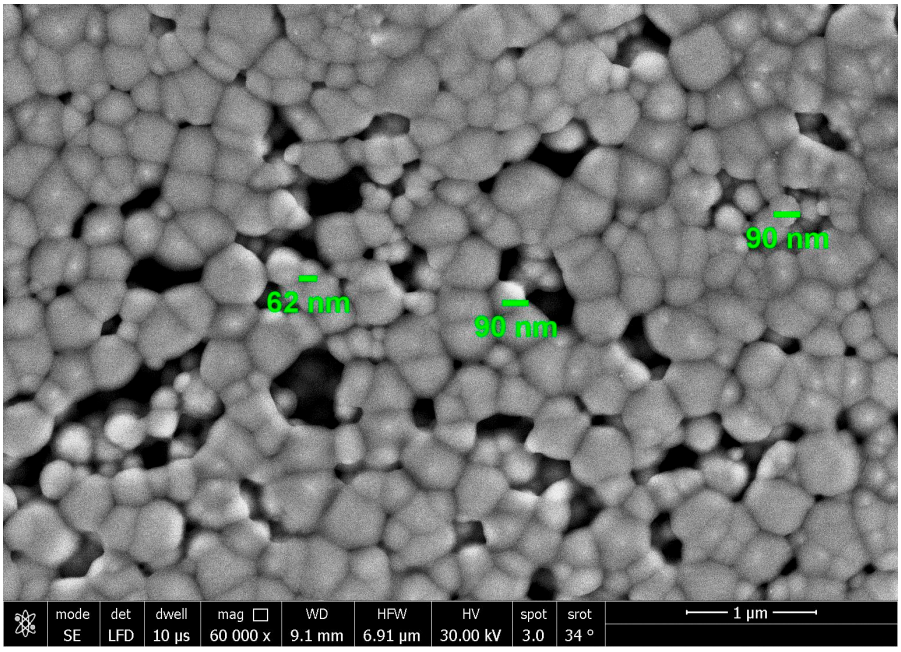


**Figure 2.** SEM image (1 µm) of magnetite nanogel.

Meanwhile, gel formation had no characteristic peaks due to its amorphous nature. The morphology illustrated by atomic force microscopy (AFM), scanning electron microscopy (SEM), and transmission electron microscopy (TEM) showed the spherical shape of MNG (Figure 1D, Figure 2, and Figure 3).

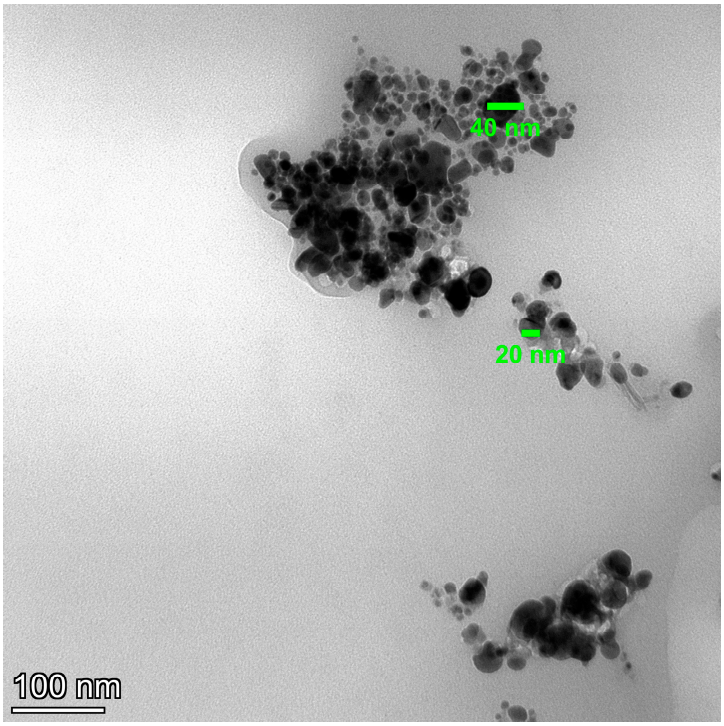


**Figure 3.** TEM image (100 nm) of magnetite nanogel.

### *2.2. Absorption of Pb Ions by MNG*

Figure 4A shows that MNG caused a dramatic drop in the concentration of Pb ions throughout all sampling points. The concentration decreased from 169.53 mg $L^{-1}$ at the beginning of the experiment to 82.87 mg $L^{-1}$ after 120 h.

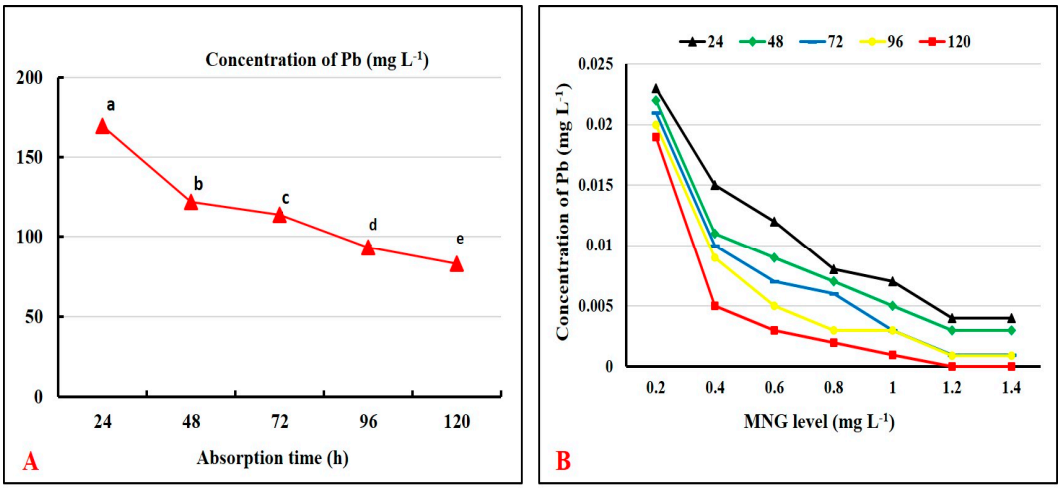


**Figure 4.** (**A**) Absorption of lead (Pb) by magnetite nanogel (MNG) across 24, 48, 72, 96, and 120 h. (**B**) Impact of MNG level on the concentration of Pb ions across 24, 48, 72, 96, and 120 h. Values that did not have the same superscripts differ significantly (one-way ANOVA; $p < 0.05$).

The various MNG concentrations affected the elimination of the Pb ions, as seen in Figure 4B. The findings showed that raising the MNG level lowered the amount of Pb ions in the aquarium water and allowed for the removal of reduced Pb metal. The outcomes also showed that 1.2 and 1.4 mg/L of MNG were the ideal doses that produced the greatest Pb ion adsorption loading.

### 2.3. Mortality and Clinical Observations

Based on Kaplan–Meier curves (Figure 5A), the survival rate was 100% in the control and MNG groups during the experimental period (45 days). The lowest survival rate was recorded in the Pb group (57.5%). There was a marked elevation in the survival rate in the MNG + Pb group (82.5%) compared with the Pb group.

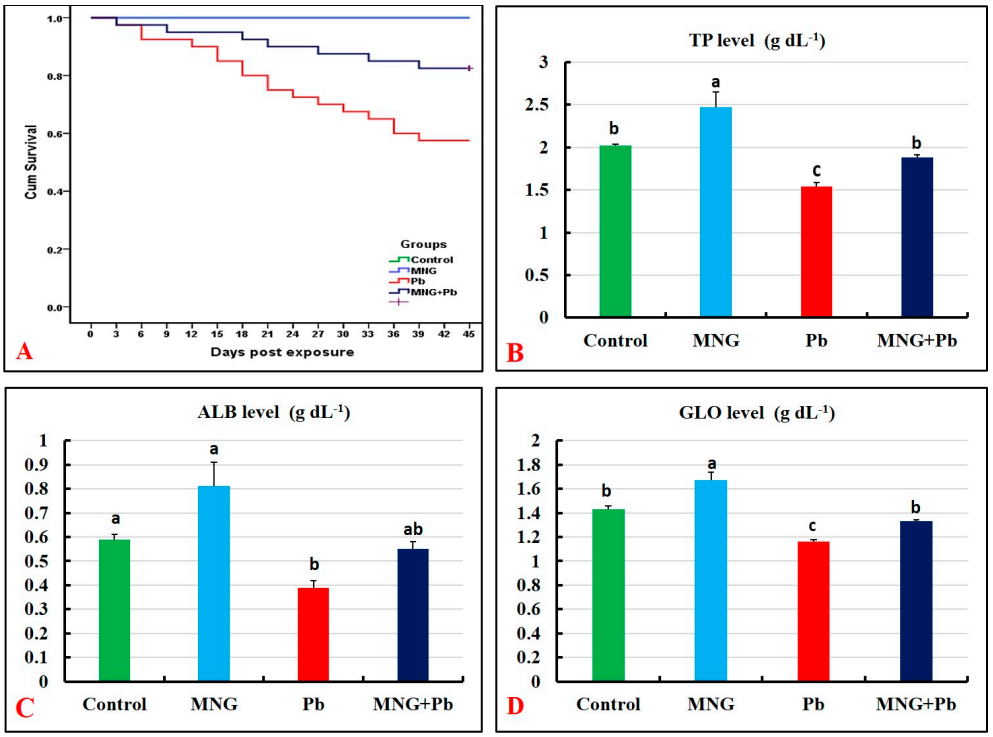


**Figure 5.** Cumulative survival ($n$ = 40/group) and protein profile parameters ($n$ = 12/group) of *C. gariepinus* exposed to magnetite nanogel (MNG) and/or lead (Pb) as a water exposure for 45 days. (**A**) Survival curves (Kaplan–Meier). (**B**) Total proteins (TP). (**C**) Albumin (ALB). (**D**) Globulins (GLO). Bars (means ± SE) that did not have the same superscripts differ significantly (one-way ANOVA; $p < 0.05$).

The clinical examination of the treated fish showed that neither the control nor the MNG groups exhibited any atypical behaviors or disease symptoms during the 45 days of exposure. On the contrary, the fish of the Pb group featured symptoms of respiratory distress manifested by rapidly moving the operculum and air gasping from the surface. Fish also developed a slimy appearance, severe skin rot, darkening, and erosions with hemorrhages. Internally, the gills were pale with congestion of internal organs. The Pb and MNG (MNG + Pb)-exposed group showed a remarkable return to the typical appearance with minimal fin rot and a mildly congested liver.

### 2.4. Hepato-Renal Function Biomarkers

Table 1 demonstrates no discernible variations in the values of hepato-renal biomarkers (ALT, AST, ALP, creatinine, and urea) between the MNG and control groups. These biomarkers displayed the highest values ($p < 0.05$) in the Pb group compared to the control. In contrast, treatment of Pb-exposed fish with MNG resulted in a significant decrease ($p < 0.05$) in these variables compared to Pb exposure alone.

**Table 1.** Liver and kidney function biomarkers of *C. gariepinus* exposed to magnetite nanogel (MNG) and/or lead (Pb) as a water exposure for 45 days ($n$ = 12/group).

| Parameters | Control | MNG | Pb | MNG + Pb |
|---|---|---|---|---|
| ALT (U $L^{-1}$) | 16.33 ± 0.93 $^{c}$ | 17.75 ± 1.91 $^{c}$ | 25.08 ± 1.17 $^{a}$ | 20.25 ± 1.23 $^{b}$ |
| AST (U $L^{-1}$) | 44.95 ± 1.22 $^{c}$ | 46.70 ± 0.85 $^{c}$ | 94.33 ± 2.20 $^{a}$ | 82.58 ± 1.68 $^{b}$ |
| ALP (U $L^{-1}$) | 34.24 ± 1.08 $^{c}$ | 34.88 ± 1.35 $^{c}$ | 50.20 ± 1.53 $^{a}$ | 41.12 ± 0.62 $^{b}$ |
| Urea (mg $dL^{-1}$) | 1.44 ± 0.05 $^{c}$ | 1.56 ± 0.04 $^{c}$ | 2.75 ± 0.10 $^{a}$ | 2.21 ± 0.05 $^{b}$ |
| Creatinine (mg $dL^{-1}$) | 0.27 ± 0.02 $^{b}$ | 0.30 ± 0.03 $^{b}$ | 0.49 ± 0.50 $^{a}$ | 0.34 ± 0.01 $^{b}$ |

ALT, alanine aminotransferase; AST, aspartate aminotransferase; ALP, alkaline phosphatase. Values (means ± SE) in the same row that did not have the same superscripts differ significantly (one-way ANOVA; $p < 0.05$).

### 2.5. Protein Profile and Immune Status

Figure 5B–D and Figure 6A–D demonstrate substantial augmentations ($p < 0.05$) in the protein profile (TP, ALB, and GLO) and immune (LYZ, C3, NO, and IgM) parameters in the MNG group related to the control. Meanwhile, the lowest concentrations of these biomarkers were observed in the Pb-exposed fish, followed by the MNG + Pb fish.

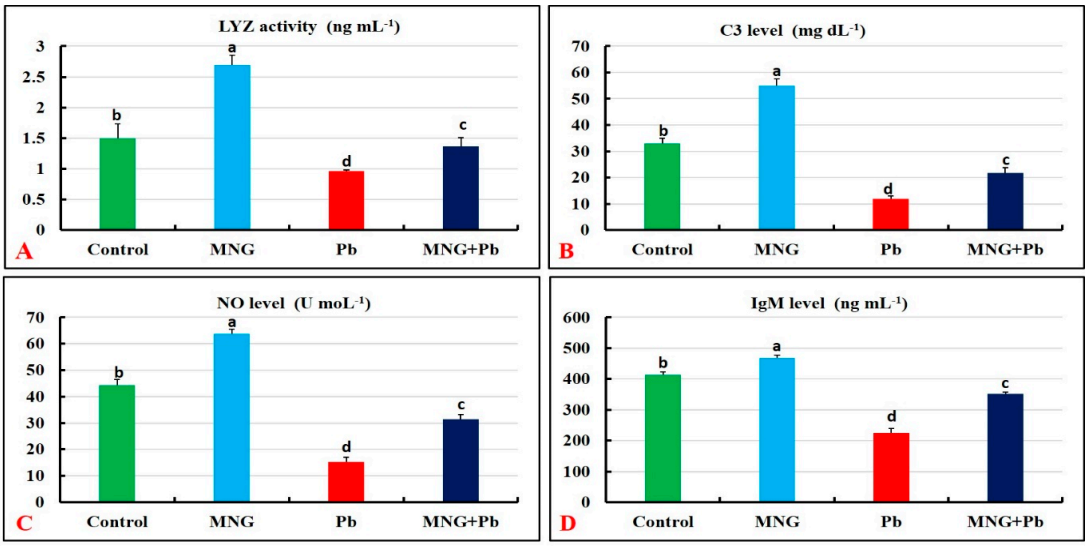


**Figure 6.** Immune parameters of *C. gariepinus* exposed to magnetite nanogel (MNG) and/or lead (Pb) as a water exposure for 45 days ($n$ = 12/group). (**A**) Lysozyme activity (LYZ). (**B**) Complement 3 (C3). (**C**) Nitric oxide (NO). (**D**) Immunoglobulin M (IgM). Bars (means ± SE) that did not have the same superscripts differ significantly (one-way ANOVA; $p < 0.05$).

### 2.6. Hepatic Oxidant/Antioxidant Status

Table 2 shows the levels of MDA and antioxidants in the liver (GSH, SOD, and CAT) of *C. gariepinus* after the exposure period (45 days). There was no noticeable variation in the MNG group's MDA level compared with the control one; however, a significant elevation ($p < 0.05$) in the GSH, SOD, and CAT values was noticed. Pb exposure induced a profound elevation in the MDA level and lessened the antioxidant values relative to the control. The values of these variables showed more improvement in the MNG + Pb group than in the Pb group.

**Table 2.** Hepatic oxidant/antioxidant biomarkers of *C. gariepinus* exposed to magnetite nanogel (MNG) and/or lead (Pb) as a water exposure for 45 days ($n$ = 12/group).

| Parameters | Control | MNG | Pb | MNG + Pb |
|---|---|---|---|---|
| MDA (nmol $mg^{-1}$) | $0.64 \pm 0.15^{c}$ | $0.99 \pm 0.05^{c}$ | $11.55 \pm 0.58^{a}$ | $3.06 \pm 0.32^{b}$ |
| GSH (ng $mg^{-1}$) | $113.57 \pm 1.84^{b}$ | $143.76 \pm 2.42^{a}$ | $41.21 \pm 0.43^{d}$ | $71.69 \pm 1.19^{c}$ |
| SOD (U $mg^{-1}$) | $88.23 \pm 1.79^{b}$ | $157.67 \pm 3.55^{a}$ | $12.73 \pm 0.49^{d}$ | $62.82 \pm 1.31^{c}$ |
| CAT (ng $mg^{-1}$) | $22.20 \pm 0.57^{b}$ | $47.30 \pm 1.65^{a}$ | $4.91 \pm 0.19^{d}$ | $8.79 \pm 0.15^{c}$ |

MDA, malondialdehyde; GSH, reduced glutathione content; SOD, superoxide dismutase; CAT, catalase. Values (means ± SE) in the same row that did not have the same superscripts differ significantly (one-way ANOVA; $p < 0.05$).

### 2.7. Histopathological Findings

According to the histopathological investigations, the livers of the control and MNG fish both displayed normal histological structures of hepatic acini and vasculatures (Figures 7A and 7B, respectively). On the contrary, the Pb exposure caused areas of fatty changes, congested hepatic blood vessels, and perivascular inflammatory cell infiltrates (Figure 7C). The livers of the MNG + Pb group exhibited an improvement of lesions as depicted by the appearance of microvacuoles within a small number of hepatocytes, congested hepatic blood vessels, inflammatory cells aggregated within the portal area, and perivascular aggregation of melanomacrophage (Figure 7D).

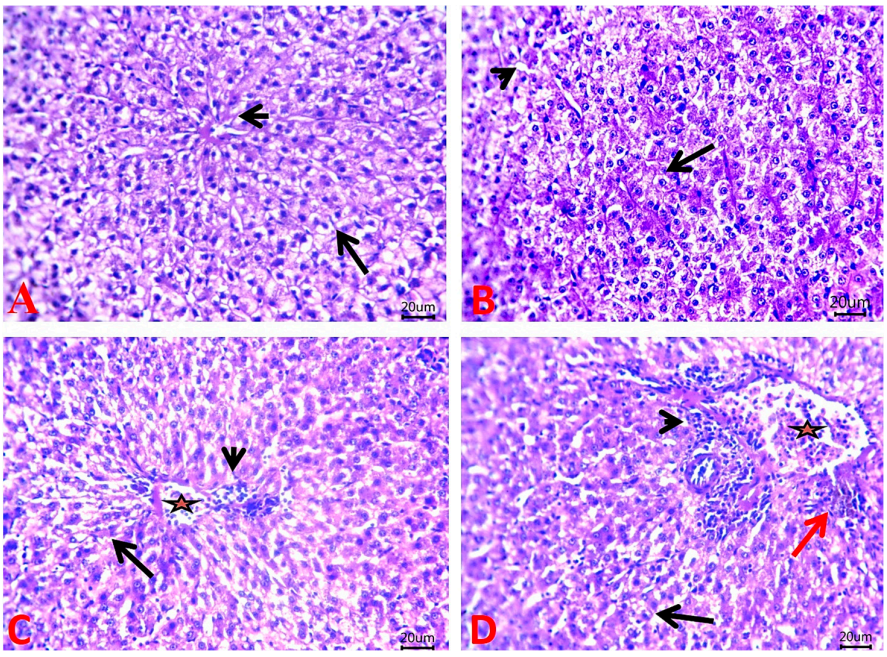


**Figure 7.** Photomicrograph of H&E-stained liver sections of *C. gariepinus* exposed to magnetite nanogel (MNG) and/or lead (Pb) as a water exposure for 45 days. (**A**,**B**) Liver of the control and MNG groups, respectively, showing normal histological structures of hepatic acini (arrow) and vasculatures (arrowheads). (**C**) Liver of the Pb group showing a focal area of fatty change (arrow), congested hepatic blood vessel (star), and perivascular inflammatory cell infiltrates (arrowhead). (**D**) Liver of the MNG +Pb group showing microvacuoles within a few numbers of hepatocytes (arrow), congested hepatic blood vessels (star), inflammatory cell aggregate within the portal area (arrowhead), and perivascular aggregation of melanomacrophage (red arrow). Scale Bar: 20 µm.

Moreover, normal renal structures with preserved glomerular capillary tufts, renal tubular epithelium, and hemopoietic cells were clear in the fish kidney of the control and MNG groups (Figures 8A and 8B, respectively). However, Pb exposure induced

histopathological alterations in the kidney, which appeared as marked necrotic changes in tubular epithelium and maintained glomerular architectures. Further, a depletion of the hemopoietic center replaced by a pale eosinophilic substance was obvious (Figure 8C). Treatment of Pb-exposed fish with MNG markedly improved these alterations and revealed normal histopathological structures of renal tubules and glomerular corpuscles (Figure 8D).

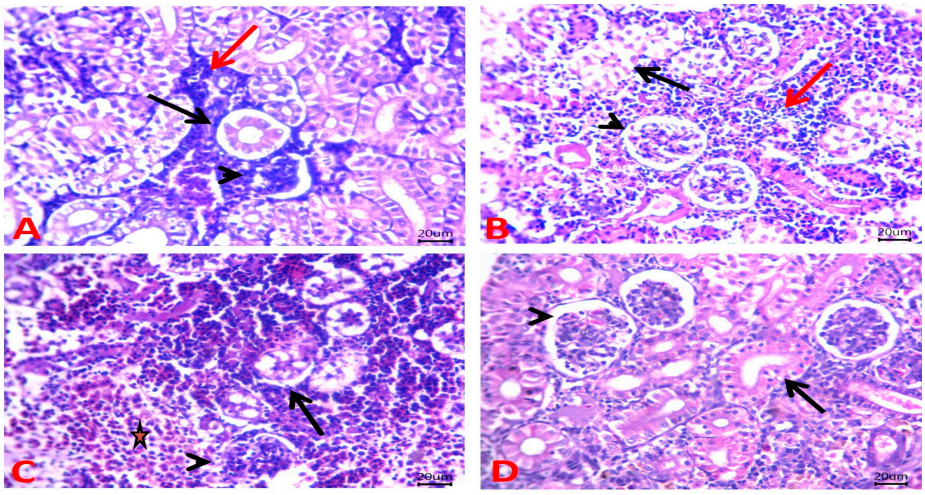


**Figure 8.** Photomicrograph of H&E-stained kidney sections of *C. gariepinus* exposed to magnetite nanogel (MNG) and/or lead (Pb) as a water exposure for 45 days. (**A**,**B**) Kidney of the control and MNG groups, respectively, showing normal renal structures with preserved glomerular capillary tufts (arrowheads), renal tubular epithelium (arrows), and the presence of hemopoietic cells (red arrows). (**C**) Kidney of the Pb group showing marked necrotic changes in the tubular epithelium (arrow), maintained glomerular architectures (arrowhead), and depletion of hemopoietic center replaced by pale eosinophilic substance (star). (**D**) Kidney of the MNG + Pb group showing normal histomorphological structures of the renal tubule (arrow) and glomerular corpuscle (arrowhead). Scale Bar: 20 µm.

### *2.8. Bioaccumulation of $Pb^{2+}$ in Fish Muscles*

The concentration of Pb ions in the muscles of the MNG and control groups did not alter significantly ($p > 0.05$), as presented in Figure 9. The muscles of the Pb group had the highest levels of Pb ions. Still, the MNG + Pb group had considerably lower levels of Pb residues.

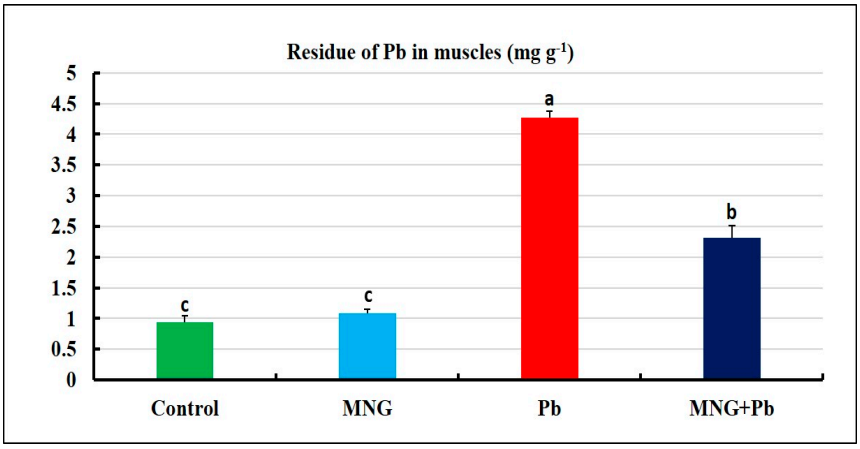


**Figure 9.** Residues of lead (Pb) in muscles of *C. gariepinus* exposed to magnetite nanogel (MNG) and/or Pb as a water exposure for 45 days ($n = 12$/group). Bars (means ± SE) that did not have the same superscripts differ significantly (one-way ANOVA; $p < 0.05$).

## 3. Discussion

The toxicity of Pb has a slow-acting cumulative impact that results in major health problems for aquatic animals and humans because of its use in various industrial processes that contaminate water [28]. The current report is an innovative trial to underpin the effectiveness of MNG to alleviate the toxicity of Pb in vitro and in vivo via assessing its magnetic power to protect fish muscles from Pb bioaccumulation and studying its potential role on protein picture, hepato-renal function, immune-antioxidant response, and tissue architecture in African catfish.

Among heavily studied nanoparticles, the magnetite nanoscale has attracted more interest owing to the potent power of magnetite to adsorb heavy metal ions in solutions. The nanosized $Fe_3O_4$ particles remove heavy metals via their magnetic properties, high surface area, chemical stability, easy synthesis, and low toxicity [29]. Pb was chosen for testing the adsorption capacity of MNG because it is one of the most predominant dangerous HMs in aquaculture practice [30]. Our findings showed that MNG had a potent adsorbing power of Pb ions that caused a clear reduction in Pb ions with time (120 h). Also, the best adsorption loading was provided by 1.2 and 1.4 mg $L^{-1}$ MNG concentrations relative to the other concentrations. The adsorption power was raised at the start of the experiment and then declined by progressing the adsorption time. These findings could be related to the adsorption and the decrease of the $Pb^{2+}$ ions to Pb metal on the surface of the MNG until the saturation of the MNG surfaces by the Pb ions. The magnetite has a specific crystal structure consisting of free electrons ($Fe^{2+}$ and $Fe^{3+}$) conjugated with oxygen. In the crystal structure, the localization of free electrons [31] is responsible for the magnetic properties, which elevate the surface activities and the adsorption power of the magnetite to lessen the Pb ions on the surface of the MNG. The sorption reaction between magnetite and Pb is chemical adsorption [32]. In the same manner, Hong et al. [33] verified the efficacy of MNG in getting rid of more than 80% of Pb, chromium (Cr), and cadmium (Cd) from contaminated water at 1 mg $L^{-1}$ because of the emerging electrostatic attraction between the positive metal ions and the negatively charged ions of iron oxide.

Considering the clinical picture and post mortem examination, exposure to Pb alters the general health of *C. gariepinus*. Additionally, fish suffered anorexia, major signs of respiratory manifestation, profound mucous secretion production, fin rot, severe erythema, erosion in the skin, and the lowest survival rate (57.5%). It is assumed that the Pb ions irritate the skin and gills because of their direct contact with fish in the aquatic environment, inducing respiratory distress and erythema with more mucous production as a defense reaction against the toxic Pb ions. Our findings were concurrent with those of Alfakheri et al. [34] and Abdel Rahman et al. [10], who noted that the exposure of *C. gariepinus* and *O. niloticus* to Pb toxicity induces respiratory problems and mortalities. On the other hand, exposure to MNG improved the clinical picture and reduced the mortalities in Pb-exposed fish. It is assumed that there are two reasons: the first is the potent magnetism of the magnetite, which enables MNG to adsorb the Pb ions, resulting in a decrease in its level. The other reason is the verified potent antioxidant activity of the NGs, which counteracts the oxidative damage produced by Pb ions. Likewise, Mahboub et al. [14] recorded no mortalities in the mercury-exposed *O. niloticus* with $Fe_3O_4$ NPs.

LYZ, complement activity, NO, and IgM are non-specific and important components that mainly indicate innate immunity in fish [35,36]. TP indicates activated humeral immunity in aquatic organisms [37]. Herein, we reveal the occurrence of immune suppression upon exposure to Pb reflected by a clear reduction in immune parameters, including lysozymes, C3, NO, IgM, and TP. Concurrent with an earlier study, Shah [38] recorded that lethal and even sub-lethal exposure to Pb alters the immunological biomarkers in tench (*Tinca tinca*). Likely, Alandiyjany et al. [12] found a clear depression in the level of TP following the exposure of *O. niloticus* to Pb.

On the other hand, immunomodulation has been reported upon the exposure of *C. gariepinus* to aqueous MNG, which is indicated by a noticeable increase in the immunological biomarkers.

The mechanism of action of $Fe_3O_4$ NPs on the immune system was recently documented by Huang et al. [39], who revealed that the degradation products of the magnetic nanoparticles improve immune stimulation via the interferon gene activating protein (STING) pathway, which, in turn, enhances cellular immune response. A similar report found that $Fe_3O_4$ NPs had an immunological influence by augmenting the activity of LYZ in *O. niloticus* exposed to mercury toxicity [14].

Detoxification of HMs is mainly carried out in the hepatic tissue, followed by filtration and excretion in the renal tissue. Hence, elevating the concentration of HMs induces an increased rate of filtration and detoxification in the fish body, which in turn causes hepato-renal dysfunction [40]. In the present investigation, the biomarkers of renal functions (creatinine and urea) and hepatic enzymes (ALT, ALP, and AST) exhibited an elevation in their levels upon exposure to Pb. It is assumed that Pb induces necrosis in the liver, and accordingly, this damage leads to the leakage of hepatic enzymes into the bloodstream, producing an elevation. Furthermore, Pb toxicity impairs renal function by minimizing its ability to excrete urine, urea and by impairing the glomerular filtration rate, as Akturk et al. [41] described. These attributions were confirmed by the histopathological alteration that was observed in the liver and kidney in our study. In line with the present findings, Abdel-Tawwab et al. [42] revealed that a noticeable increase in the values of urea and creatinine was recorded in *O. niloticus* after intoxication with a mixture of HMs, including Pb. Histological alterations of the liver and gill tissue of *C. gariepinus* were reported post-exposure to Pb, including fibrosis of hepatic cords and necrosis of parenchyma cells besides collapsing blood vessels [43].

On the other side, a restoration of hepato-renal biomarkers in the aqueous MNG + Pb-treated group and a clear regeneration of histological changes indicated the protective effect of MNG against Pb-induced hepato-renal damages. It is suggested that aqueous MNG can mitigate the hazardous effects of Pb toxicity by lessening the Pb-generated reactive oxygen species (ROS) on hepatic cells. Similarly, Mahboub et al. [14] reported that $Fe_3O_4$ NPs had a promising effect on improving hepato-renal functions of *O. niloticus* and could enhance the levels of liver enzymes and renal parameters upon exposure to mercury toxicity. A recent study conducted by Alandiyjany et al. [12] reported severe histopathological changes in the liver and gills of *O. niloticus* following exposure to Pb, and a noticeable improvement was detected in the magnetized silica-received group.

HMs induce oxidative damage by generating ROS. The antioxidant defense mechanism involves various enzymes, such as CAT, SOD, and GSH, which protect cells from oxidative stress by detoxifying ROS [44]. The current work showed that oxidative damage in the Pb-exposed group reflected a clear elevation in MDA level and a reduction in GSH, CAT, and SOD. It is opined that Pb causes excess production of ROS, resulting in oxidative damage. In line with recent work, Alandiyjany et al. [12] detected decreased serum CAT, SOD, and GSH activity levels in Pb-exposed *O. niloticus*.

Contrarily, the exposure of fish to MNG in the Pb-exposed group has an antioxidant-protecting effect indicated by a clear modulation in the antioxidant biomarkers (elevated SOD and CAT activities) resulting in protection from oxidative damage. In line with a recent finding, Răcuciu et al. [45] confirmed that $Fe_3O_4$ NPs have potent antioxidant enzymatic activity via modulating the levels of CAT and SOD and aid in plant development. Moreover, $Fe_3O_4$ NPs can enhance the antioxidant status and reduce the oxidative stress of *O. niloticus* and Indian major carp (*Labeo rohita*) [14,46,47].

HM toxicity produces variable immunological and physiological responses, allowing for the bioaccumulation of metals in different fish tissues [7]. Here, we find that the Pb-exposed group's muscles have a greater level of Pb. In line with a recent report, Alandiyjany et al. [12] detected bioaccumulation of Pb in the muscles of *O. niloticus* following exposure to Pb.

In contrast, the MNG + Pb group reflected the least accumulation of Pb, indicating its efficacy in removing Pb. It is assumed that the magnetic power of magnetite found in MNG, plus the formulation of NGs, enables it to absorb Pb strongly. Previous studies

supported our outcomes and documented that the structure of NGs causes them to be easily biocompatible and biodegradable and can absorb and release molecules for decontaminating water, catalysis, and sensors [48,49]. Furthermore, Neamtu et al. [50] added that NGs can absorb active materials through chemical interactions such as hydrogen or hydrophobic bonding and salt formation. Similar outcomes were observed by Alandiyjany et al. [12] in the muscles of *O. niloticus.*

## 4. Conclusions

The present study demonstrates that Pb is a hazardous heavy metal that causes a decline in the survival rate, suppresses immune-antioxidant status, and deteriorates hepato-renal functions and histopathological structure of the liver and kidney tissues. Also, Pb exposure results in high bioaccumulation in the muscles of the treated African catfish. The basic attention is directed to the magnetic antitoxic power of MNG to adsorb Pb ions and protect fish from bioaccumulation in muscles. Additionally, MNG enhances the immune-antioxidant profile, improves the hepato-renal function, and regenerates the histopathological picture. Further studies are mandatory to assess other applications of MNG in various fish species and to assess the safe use on a large scale for sustaining aquaculture and maintaining human health.

## 5. Materials and Methods

### *5.1. Synthesis and Characterization of MNG*

Firstly, $Fe_3O_4$ NPs were synthesized following the protocol of Hamdy et al. [51]. About 0.4 g of the hematite ore ($Fe_3O_4$) was added drop by drop to 40 mL of $H_2O_2$. At the same time, the mixture was subjected to ultrasound at 60 kHz for 2.5 h in an ultrasonic device (Sonica 4200 EPS3, Milano, Italy) until the black particles of $Fe_3O_4$ were obtained. After 1.5 h, the $Fe_3O_4$ NPs (black color) precipitated from the supernatant (reddish color). The $Fe_3O_4$ NPs were separated from the solution by centrifugation at 4000 rpm, and, finally, the $Fe_3O_4$ NPs were washed four times using methanol.

For the synthesis of $Fe_3O_4$ NPs/carbopol hybrid nanogel, 0.2 g of $Fe_3O_4$ NP desperation in 25 mL of ethanol was added to a solution of 0.25 g carbopol dissolved in 25 mL of ethanol and the mixture was stirred using a mechanical stirrer for 50 min. Then, 0.75 mL of trimethylamine was added drop by drop and stirred for another 40 min until obtaining a black gel. The $Fe_3O_4$ NPs/carbopol hybrid nanogel was prepared in high and low viscosities.

Characterization protocols were categorized into three groups: morphology, identification, and index class, according to the Hassan et al. [52] approach.

### *5.2. Preparation of Pb Ion Solution*

In this experiment, lead chloride ($PbCl_2$; purity 98%) of Merck, Darmstadt, Germany was utilized as a source of Pb ions. To reach the proper concentrations, $PbCl_2$ was primarily dissolved in de-ionized water to create a stock solution (1000 mg $L^{-1}$) which was then diluted to the necessary concentration before being used in aquarium water. According to Alfakheri et al. [34], the 96 h median lethal concentration ($LC_{50}$) for Pb was 231 mg $L^{-1}$ and 30% of 96 h $LC_{50}$ (69.30 mg $L^{-1}$) was used.

### *5.3. Adsorption Capacity of MNG*

In two different studies, the capacity of MNG to adsorb the Pb ions was evaluated. In the first experiment, at 24 °C and pH 6.0, an exact amount of $PbCl_2$ (20 mg) was mixed with 100 mL of ultrapure water. In a glass vial, 20 mL of prepared $PbCl_2$ and 20 mg of MNG were mixed and vortexed for 10 min to assess the adsorption kinetics per the Kôsak et al. [53] technique. Daily, for five days (24, 48, 72, 96, and 120 h), and using an atomic absorption spectrophotometer (Buck Scientific, Norwalk, CT, USA), the concentration of $Pb^{+2}$ ions was calculated. Three copies of each sample were tested.

The second experiment examined how varied MNG concentrations (0.2, 0.4, 0.6, 0.8, 1, 1.2, and 1.4 mg $L^{-1}$) affected the adsorption ability of Pb ions. It involved setting up seven aquariums with water in them, adding 0.025 mg $L^{-1}$ of Pb ions to each aquarium at pH 6.0, and then adding the seven concentrations of MNG directly to each Pb-exposed aquarium [4]. Then, using the atomic absorption spectrophotometry technique, the level of Pb ions was assessed after 24, 48, 72, 96, and 120 h. The safe recommended level of iron in fish, which varies between 0.35 and 1.7 mg/L [54,55], was considered when choosing the concentrations of MNG.

### 5.4. Ethical Agreement and Fish Acclimation

The Institutional Animal Care and Use Committee of Zagazig University in Egypt (ZU-IACUC/2/F/309/2022) approved the experimental strategy. Two hundred and forty African catfish (100 ± 7.39 g) were selected from the Al-Abbassa private fish farm in Sharkia Governorate, Egypt. The fish were kept for ten days in 100 L of well-aerated aquaria for acclimation. Part of the water was partially exchanged (25%). The fish were supplemented with a basal diet at 3% of their body weight twice daily during acclimation and experimental trial. Assessment of physio-chemical parameters of the rearing water was carried out daily, including temperature, dissolved oxygen, ammonia, and pH, and recorded as 24 ± 2 °C, 6 ± 0.26 mg $L^{-1}$, 0.01 ± 0.04 mg $L^{-1}$, and 7 ± 0.13, respectively.

### 5.5. Assessing the Initial Concentration of MNG

Fish ($n$ = 80) were exposed to 8 various concentrations of MNG for 15 days (Table 3) to determine the starting concentration for the treatment experiment. These concentrations were 0, 0.2, 0.4, 0.6, 0.8, 1, 1.2, and 1.4 mg $L^{-1}$ of MNG. The clinical observations were kept track of every day during the preliminary trial. MNG concentrations were safe in the 0.2 to 1.4 mg $L^{-1}$ range, and 1.2 mg $L^{-1}$ was determined to be the dose used for treatment.

**Table 3.** Mortality and clinical observations of *C. gariepinus* exposed to different concentrations of magnetite nanogel (MNG) for 15 days.

| Conc. (mg $L^{-1}$) | Mortality ($n$ = 10) | Clinical Observations | | |
|---|---|---|---|---|
| | | Erratic Swimming | Loss of Escape Reflex | External Symptoms (Hemorrhages, Darkness, Fin Rot, and Ulcerations) |
| 0.0 | 0/10 | - | - | - |
| 0.2 | 0/10 | - | - | - |
| 0.4 | 0/10 | - | - | - |
| 0.6 | 0/10 | - | - | - |
| 0.8 | 0/10 | - | - | - |
| 1 | 0/10 | - | - | - |
| 1.2 | 0/10 | - | - | - |
| 1.4 | 0/10 | - | - | - |

(-) No abnormal observations.

### 5.6. Experimental Design

For 45 days, fish ($n$ = 160) were randomly assigned into four groups (10 fish/replicate; 40/group). The first and second (MNG) groups were exposed to 0 and 1.2 mg/L MNG in water, where the control was the first group. The third (Pb) and fourth (MNG + Pb) groups were exposed to 0 and 1.2 mg $L^{-1}$ MNG in water, respectively, and 69.30 mg $L^{-1}$ of lead chloride. Fish were moved to freshly produced solutions with the same concentrations daily for 45 days during the experiment. Every day, about 25% of the aquarium's contents were replenished. Clinical observation and mortalities were kept track of throughout the trial.

### 5.7. Sampling

Fish were randomly selected (12 fish per group) at the end of the experiment (45 days) to collect samples. According to Neiffer and Stamper's [56] approach, fish were anesthetized with a benzocaine solution (100 mg $L^{-1}$), and blood was then drained from the caudal blood vessels using tubes devoid of the anticoagulant. Samples were centrifuged at 1750× *g* for 10 min after being incubated at room temperature (21 ± 3 °C) for 5 h. Clear serum was then kept at 20 °C until biochemical and immunological assays. Liver tissues (12 fish/group) were gathered and kept in liquid nitrogen for the oxidant/antioxidant assay. Additionally, liver and kidney samples (12 fish/group) were used for histopathology analysis, and samples of muscles (12 fish/group) were picked for determining Pb residues.

### 5.8. Evaluation of Hepato-Renal Function Biomarkers

The activity of hepatic function biomarkers, including aspartate aminotransferase (AST, Catalog No.; EK12276) (Biotrend Co., Laurel, MD, USA), alanine aminotransferase (ALT, Catalog No.; MBS038444) (MyBioSource Co., CA, USA), and alkaline phosphatase (ALP, Catalog No.; TR11320) (Thermo Fisher Scientific, Swindon, UK) were computed. Also, the total protein (TP, Catalog No.; MBS9917835), albumin (ALB, Catalog No.; MBS019237), and urea (Catalog No.; MBS9374784) (MyBioSource Co., CA, USA) were measured. All the biomarkers mentioned above were computed using a spectrophotometer (Lambda EZ201; Perkin Elm, Beaconsfield, UK). The globulin (GLO) level was determined by subtracting ALB from TP. The creatinine (Catalog No.; MAC080) level was estimated at a wavelength of 340 nm using a spectrophotometric protocol (Centromic Gmbit kit manual, Wartenberg, Germany).

### 5.9. Immune Assays

The immune parameters, including lysozyme activity (LYZ), were estimated using the inhibition zone method in agarose gel plates, depending on the protocol of Lee and Yang [57]. The level of complement 3 (C3) was measured by immunoturbidimetry using the method of Abdollahi et al. [58] with separated Eastbiopharm ELISA kits (Hangzhou Eastbiopharm CO., LTD., Torrance, CA, USA).

To quantify the serum nitric oxide (NO), about 100 mL of each serum sample was added to the Griess reagent, which was then incubated for 10 min at 27 °C [59]. Immunoglobulin M (IgM) was quantified in serum spectrophotometrically using ELISA kits (Cusabio Biotech Co., Ltd., Wuhan, China) as directed by the manufacturer, following Schultz's [60] approach.

### 5.10. Hepatic Oxidant/Antioxidant Assays

According to the Siroka et al. [61] assay, the liver samples were prepared to estimate the levels of oxidant/antioxidant biomarkers (malondialdehyde (MDA), reduced glutathione content (GSH), catalase (CAT), and superoxide dismutase (SOD)). Liver samples were subjected to homogenization in a buffer with a pH of 7.5 to obtain the supernatant, which was then obtained by centrifuging them at 4 °C for 15 min at 10,000 × *g* for 1 h to recover the final supernatant.

The level of MDA was assessed using the Sigma assay kit (MAK085) according to the protocol of Ohkawa et al. [62]. The content of GSH and SOD activity was computed depending on the assays of Beutler et al. [63] and Velkova-Jordanoska et al. [64]. The GSH was estimated at 412 nm using 5,5′-dithio-bis-2-nitrobenzoic acid in the supernatant fraction. The level of SOD was calculated using the xanthine oxidase–cytochrome protocol using a spectrophotometer at 505 nm. Xanthine interacted with 2-[4-iodophenyl]-3-[4-nitrophenyl]-5-phenyl-tetrazolium chloride (INT) to compose superoxide radicals producing red-colored formazan. This product was utilized to measure the activity of SOD as SOD conjugate with superoxide radicals and consequently controls the formazan synthesis.

The activity of CAT was monitored depending on the decrease in hydrogen peroxide ($H_2O_2$) at 240 nm using a light plate and a spectrophotometer with 1.0 mL quartz cuvettes according to the method of Aksenes and Njaa [65].

### *5.11. Histopathological Investigation*

Samples from the liver and kidneys were gathered from all investigated groups, fixed using 10% buffered neutral formalin, then exposed to dehydration in ascending degrees of alcohol, cleared using xylene, and soaked in paraffin. Paraffin sections of about 5 µm in thickness were arranged and stained using hematoxylin and eosin (H&E) and then inspected by an optical microscope, depending on the protocol of Suvarna et al. [66].

### *5.12. Determination of Pb Residues in Fish Muscles*

After terminating the experiment (45 days), representative samples were dissected from the dorsal muscle of each group and dried in an oven at 85 °C until they reached a stabilized weight. The prepared samples were weighed (1 g dry weight) and placed in a muffle furnace (Shelton, CT, USA) for 6 h of ashing. After the procedure outlined by Golberg et al. [67], the samples were digested using 5 mL of freshly made perchloric acid ($HCLO_4$; 70%) and nitric acid ($HNO_3$; 65% $v/v$) to Teflon beakers and heating at 50 °C for approximately 5 h to completely break down the organic matter. The digested solution was chilled at ~21 ± 2 °C and diluted using deionized water to reach a final volume of 50 mL. The atomic absorption spectrophotometer was used to analyze each sample separately for calculating the Pb ion residues [68].

### *5.13. Data Analysis*

The Shapiro–Wilk test was first conducted to evaluate whether all the data were normal. To determine whether there was a statistically significant difference between treatments, a one-way analysis of variance (ANOVA) was performed with Tukey's post hoc analysis (SPSS version 18; IBM Corp., Armonk, NY, USA). The Kaplan–Meier protocol was used to analyze survival according to Kaplan and Meier [69]. A $p$-value of less than 0.05 represents statistical variance, including all tests.

**Author Contributions:** Conceptualization, A.N.A.R., A.T.M. and H.H.M.; Methodology, A.N.A.R., B.A.E., A.T.M., H.M.A.-G., E.M.M.Y., A.E., K.M.A., S.H.I. and H.H.M.; Software and data curation: A.N.A.R., S.H.I. and H.H.M.; Writing—Original draft preparation: A.N.A.R. and H.H.M.; Writing—Reviewing and Editing: A.N.A.R., A.T.M. and H.H.M.; Funding acquisition, K.M.A. All authors have read and agreed to the published version of the manuscript.

**Funding:** The APC was funded by Princess Nourah bint Abdulrahman University Researchers Supporting Project number (PNURSP2023R402), Princess Nourah bint Abdulrahman University, Riyadh, Saudi Arabia. This work was supported by the Deanship of Scientific Research, Vice Presidency for Graduate Studies and Scientific Research, King Faisal University, Saudi Arabia (Grant No. GRANT 3867).

**Institutional Review Board Statement:** The experimentation was performed in the Aquatic Animal Medicine Department, Faculty of Veterinary Medicine, Zagazig University, and supervised by the Animal Use in Research Committee with ethical approval code ZU-IACUC/2/F/309/2022. All experimental procedures were conducted in compliance with the ethical guidelines approved by the National Institutes of Health for the Use and Treatment of Laboratory Animals.

**Informed Consent Statement:** Not applicable.

**Data Availability Statement:** The datasets generated or analyzed during the current study are not publicly available but are available from the corresponding author upon reasonable request.

**Acknowledgments:** The authors appreciate Princess Nourah bint Abdulrahman University Researchers Supporting Project number (PNURSP2023R402), Princess Nourah bint Abdulrahman University, Riyadh, Saudi Arabia. This work was supported by the Deanship of Scientific Research, Vice Presidency for Graduate Studies and Scientific Research, King Faisal University, Saudi Arabia (Grant No. GRANT 3867). We also would like to thank all staff of Aquatic Animal Medicine, Faculty of Veterinary Medicine, Zagazig University, for their kind support during the study.

**Conflicts of Interest:** The authors declare no conflict of interest.

## References


1. Yap, C.K.; Al-Mutairi, K.A. Ecological-health risk assessments of heavy metals (Cu, Pb, and Zn) in aquatic sediments from the ASEAN-5 emerging developing countries: A review and synthesis. *Biology* **2022**, *11*, 7. [CrossRef] [PubMed]
2. Feng, W.; Wang, Z.; Xu, H. Species-specific bioaccumulation of trace metals among fish species from Xincun Lagoon, South China Sea. *Sci. Rep.* **2020**, *10*, 21800. [CrossRef] [PubMed]
3. Bella, C.D.; Calagna, A.; Cammilleri, G.; Chembri, P.; Monaco, D.L.; Ciprì, V.; Battaglia, L.; Barbera, G.; Ferrantelli, V.; Sadok, S.; et al. Risk assessment of cadmium, lead, and mercury on human health in relation to the consumption of farmed sea bass in Italy: A meta-analytical approach. *Front. Mar. Sci.* **2021**, *8*, 616488. [CrossRef]
4. El-Bouhy, Z.M.; Reda, R.M.; Mahboub, H.H.; Gomaa, F.N. Bioremediation effect of pomegranate peel on subchronic mercury immunotoxicity on African catfish, *Clarias gariepinus*. *Environ. Sci. Pollut. Res.* **2021**, *28*, 2219–2235. [CrossRef]
5. El-Bouhy, Z.M.; Reda, R.M.; Mahboub, H.H.; Gomaa, F.N. Chelation of mercury intoxication and testing different protective aspects of *Lactococcus lactis* probiotic in African catfish. *Aquaculture Res.* **2021**, *52*, 3815–3828. [CrossRef]
6. Apiamu, A.; Osawaru, S.U.; Asagba, S.O.; Evuen, U.F.; Achuba, F.I. Exposure of African catfish (*Clarias gariepinus*) to lead and zinc modulates membrane-bound transport protein: A plausible effect on Na+/K+-ATPase activity. *Biol. Trace Elem. Res.* **2022**, *200*, 4160–4170. [CrossRef]
7. Garai, P.; Banerjee, P.; Mondal, P.; Saha, N.C. Effect of heavy metals on fishes: Toxicity and bioaccumulation. *J. Clin. Toxicol.* **2021**, *18*, S18:001. [CrossRef]
8. Lee, J.W.; Choi, H.; Hwang, U.K.; Kang, J.C.; Kang, Y.J.; Kim, K.I. Toxic effects of lead exposure on bioaccumulation, oxidative stress, neurotoxicity, and immune responses in fish: A review. *Environ. Toxicol. Pharmacol.* **2019**, *68*, 101–108. [CrossRef]
9. Abdel-Warith, A.A.; Younis, E.M.I.; Al-Asgah, N.A.; Rady, A.M.; Allam, H.Y. Bioaccumulation of lead nitrate in tissues and its effects on hematological and biochemical parameters of *Clarias gariepinus*. *Saudi J. Biol. Sci.* **2020**, *27*, 840–845. [CrossRef]
10. Abdel Rahman, A.N.; ElHady, M.; Hassanin, M.E.; Mohamed, A.A.R. Alleviative effects of dietary Indian lotus leaves on heavy metals-induced hepato-renal toxicity, oxidative stress, and histopathological alterations in Nile tilapia, *Oreochromis niloticus* (L.). *Aquaculture* **2019**, *509*, 198–208. [CrossRef]
11. Mahboub, H.H.; Shahin, K.; Mahmoud, S.M.; Altohamy, D.E.; Husseiny, W.A.; Mansour, D.A.; Shalaby, S.I.; Gaballa, M.M.S.; Shaalan, M.; Alkafafy, M.; et al. Silica nanoparticles are novel aqueous additive mitigating heavy metals toxicity and improving the health of African catfish, *Clarias gariepinus*. *Aquat. Toxicol.* **2022**, *249*, 106238. [CrossRef]
12. Alandiyjany, M.N.; Kishawy, A.T.Y.; Hassan, A.A.; Eldoumani, H.; Elazab, S.T.; El-Mandrawy, S.A.M.; Saleh, A.A.; El Sawy, N.A.; Attia, Y.A.; Arisha, A.H.; et al. Nano-silica and magnetized-silica mitigated lead toxicity: Their efficacy on bioaccumulation risk, performance, and apoptotic targeted genes in Nile tilapia (*Oreochromis niloticus*). *Aquat. Toxicol.* **2022**, *242*, 106054. [CrossRef]
13. Abdel Rahman, A.N.; Ismail, S.H.; Fouda, M.M.S.; Abdelwarith, A.A.; Younis, E.M.; Khalil, S.S.; El-Saber, M.M.; Abdelhamid, A.E.; Davies, S.J.; Ibrahim, R.E. Impact of *Streptococcus agalactiae* challenge on immune response, antioxidant status and hepatorenal indices of Nile tilapia: The palliative role of chitosan white poplar nanocapsule. *Fishes* **2023**, *8*, 199. [CrossRef]
14. Mahboub, H.H.; Beheiry, R.R.; Shahin, S.E.; Behairy, A.; Khedr, M.H.E.; Ibrahim, S.M.; Elshopakey, G.E.; Daoush, W.M.; Altohamy, D.E.; Ismail, T.A.; et al. Adsorptivity of mercury on magnetite nano-particles and their influences on growth, economical, hemato-biochemical, histological parameters and bioaccumulation in Nile tilapia (*Oreochromis niloticus*). *Aquat. Toxicol.* **2021**, *235*, 105828. [CrossRef]
15. Kavas, H.; Günay, M.; Baykal, A.; Toprak, M.S.; Sozeri, H.; Aktaş, B. Negative Permittivity of Polyaniline-$Fe_3O_4$ Nanocomposite. *J. Inorg. Organomet. Polym. Mater.* **2013**, *23*, 306–314. [CrossRef]
16. Shaker, S.; Zafarian, S.; Chakra, C.S.; Rao, K.V. Preparation and characterization of magnetite nanoparticles by sol-gel method for water treatment. *Int. J. Innov. Res. Technol. Sci. Eng.* **2013**, *2*, 2969–2973.
17. Lemine, O.M.; Omri, K.; Zhang, B.; El Mir, L.; Sajieddine, M.; Alyamani, A.; Bououdina, M. Sol–gel synthesis of 8nm magnetite ($Fe_3O_4$) nanoparticles and their magnetic properties. *Superlattices Microstruct.* **2012**, *52*, 793–799. [CrossRef]
18. Cui, H.; Liu, Y.; Ren, W. Structure switch between α-$Fe_2O_3$, γ-$Fe_2O_3$ and $Fe_3O_4$ during the large scale and low temperature sol—Gel synthesis of nearly monodispersed iron oxide nanoparticles. *Adv. Powder Technol.* **2013**, *2*, 93–97. [CrossRef]
19. Neyaz, N.; Zarger, M.S.; Siddiq, W.A. Synthesis and characterisation of modified magnetite super paramagnetic nano composite for removal of toxic metals from ground water. *Int. J. Environ. Sci.* **2014**, *5*, 260–269. Available online: https://www.cabdirect.org/cabdirect/abstract/20153136507 (accessed on 6 July 2023).
20. Zhang, H.; Zhai, Y.; Wang, J. New progress and prospects: The application of nanogel in drug delivery. *Mater. Sci. Eng. C* **2016**, *60*, 560–568. [CrossRef]
21. Kaoud, R.M.; Heikal, E.J.; Jaafar, L.M. Novel nanogel applications: A review. *WJAHR* **2022**, *6*, 11–15.
22. Pinellia, F.; Saadatia, M.; Zareb, E.N.; Makvandic, P.; Masia, M.; Filippo, A.S. A perspective on the applications of functionalized nanogels: Promises and challenges. *Int. Mater. Rev.* **2023**, *68*, 1–25. [CrossRef]
23. Anandharamakrishnan, C. Trends and impact of Nanotechnology in agro-Food sector. In *Innovative Food Processing Technologies*; Knoerzer, K., Muthukumarappan, K., Eds.; Elsevier: Oxford, UK, 2021; pp. 523–531. [CrossRef]
24. Yiamsawas, D.; Kangwansupamonkon, W.; Kiatkamjornwong, S. Lignin-based nanogels for therelease of payloads in alkaline conditions. *Eur. Polym. J.* **2021**, *145*, 110241. [CrossRef]
25. Shoueir, K.R.; Sarhan, A.A.; Atta, A.M. Macrogel andnanogel networks based on crosslinked poly (vinylalcohol) for adsorption of methylene blue from aquasystem. *Environ. Nanotechnol. Monit. Manag.* **2016**, *5*, 62–73. [CrossRef]

26. Shah, M.T.; Alveroglu, E. Facile synthesis of nanogelsmodified $Fe_3O_4$@Ag NPs for the efficient adsorption of bovine & human serum albumin. *Mater. Sci. Eng. C* **2021**, *118*, 111390. [CrossRef]
27. Abdulhady, Y.A.; El-Shazly, M.M. Removal of some heavy metals and polluted antibacterial activities via synthesized magnetic nano-composite of iron oxide and derivatives: Chemical and microbial treatment case study: Al tard-bilraha drain Ismailia, EGYPT. *Egypt J. Desert Res.* **2018**, *68*, 15–36. [CrossRef]
28. Raj, L.; Das, A.P. Lead pollution: Impact on environment and human health and approach for a sustainable solution. *J. Environ. Chem. Ecotoxicol.* **2023**, *5*, 79–85. [CrossRef]
29. Sarma, G.K.; Sen Gupta, S.; Bhattacharyya, K.G. Nanomaterials as versatile adsorbents for heavy metal ions in water: A review. *Environ. Sci. Poll. Res.* **2019**, *26*, 6245–6278. [CrossRef]
30. Emenike, E.C.; Iwuozor, K.O.; Anidiobi, S.U. Heavy metal pollution in aquaculture: Sources, impacts and mitigation techniques. *Biol. Trace Elem. Res.* **2022**, *200*, 4476–4492. [CrossRef]
31. Daoush, W.M. Co-precipitation and magnetic properties of magnetite nanoparticles for potential biomedical applications. *J. Nanomed. Res.* **2017**, *5*, 118–123. [CrossRef]
32. Rajput, S.; Pittman, C.U.; Mohan, D. Magnetic magnetite (Fe3O4) nanoparticle synthesis and applications for lead ($Pb^{2+}$) and chromium (Cr6+) removal from water. *J. Colloid Interface Sci.* **2016**, *468*, 334–346. [CrossRef]
33. Hong, J.; Xie, J.; Mirshahghassemi, S.; Lead, J. Metal (Cd, Cr, Ni, Pb) removal from environmentally relevant waters using polyvinylpyrrolidone-coated magnetite nanoparticles. *RSC Adv.* **2020**, *10*, 3266–3276. [CrossRef]
34. Alfakheri, M.; Elarabany, N.; Bahnasawy, M. Effects of lead on some oxidative stress of the African catfish, *Clarias gariepinus*. *J. Egypt. Acad. Soc. Environ. Dev.* **2018**, *19*, 171–175. [CrossRef]
35. Ibrahim, R.E.; Elshopakey, G.E.; Abd El-Rahman, G.I.; Ahmed, A.I.; Altohamy, D.E.; Zaglool, A.W.; Younis, E.M.; Abdelwarith, A.A.; Davies, S.J.; Al-Harthi, H.F. Palliative role of colloidal silver nanoparticles synthetized by moringa against *Saprolegnia* spp. infection in Nile Tilapia: Biochemical, immuno-antioxidant response, gene expression, and histopathological investigation. *Aquac. Rep.* **2022**, *26*, 101318. [CrossRef]
36. Abdel Rahman, A.N.; Elshopakey, G.E.; Behairy, A.; Altohamy, D.E.; Ahmed, A.I.; Farroh, K.Y.; Alkafafy, M.; Shahin, S.A.; Ibrahim, R.E. Chitosan-*Ocimum basilicum* nanocomposite as a dietary additive in *Oreochromis niloticus*: Effects on immune-antioxidant response, head kidney gene expression, intestinal architecture, and growth. *Fish Shellfish Immunol.* **2022**, *128*, 425–435. [CrossRef]
37. Alexander, C.; Sahu, N.; Pal, A.; Akhtar, M. Haemato-immunological and stress responses of *Labeo rohita* (Hamilton) fingerlings: Effect of rearing temperature and dietary gelatinized carbohydrate. *J. Anim. Physiol. Anim. Nutr.* **2011**, *95*, 653–663. [CrossRef]
38. Shah, S.L. Alterations in the immunological parameters of tench (*Tinca tinca* L. 1758) after acute and chronic exposure to lethal and sublethal treatments with mercury, cadmium and lead. Turkish. *J. Vet. Anim. Sci.* **2005**, *29*, 1163–1168.
39. Huang, L.; Liu, Z.; Wu, C.; Lin, J.; Liu, N. Magnetic nanoparticles enhance the cellular immune response of dendritic cell tumor vaccines by realizing the cytoplasmic delivery of tumor antigens. *Bioeng. Transl. Med.* **2023**, *8*, e10400. [CrossRef]
40. Soto, M.; Marigomez, I.; Cancio, I. *Biological Aspects of Metal Accumulation and Storage*; University of the Basque Country: Leioa, Spain, 2003.
41. Akturk, O.; Demirin, H.; Sutcu, R.; Yilmaz, N.; Koylu, H.; Altuntas, I. The effects of diazinon on lipid peroxidation and antioxidant enzymes in rat heart and ameliorating role of vitamin E and vitamin C. *Cell Biol. Toxicol.* **2006**, *22*, 455–461. [CrossRef]
42. Abdel-Tawwab, M.; El-Sayed, G.O.; Monier, M.N.; Shady, S.H. Dietary EDTA supplementation improved growth performance, biochemical variables, antioxidant response, and resistance of Nile tilapia, *Oreochromis niloticus* (L.) to environmental heavy metals exposure. *Aquaculture* **2017**, *473*, 478–486. [CrossRef]
43. Olojo, E.A.A.; Olurin, K.B.; Mbaka, G.; Oluwemimo, A.D. Histopathology of the gill and liver tissues of the African catfish *Clarias gariepinus* exposed to lead. *African J. Biotechnol.* **2005**, *4*, 117–122.
44. Mondal, P.; Garai, P.; Chatterjee, A.; Saha, N.C. Toxicological and therapeutic effects of neem (*Azadirachta indica*) leaf powder in hole-in-the-head (HITH) disease of fish *Anabas testudineus*. *Aquac Res.* **2020**, *52*, 715–723. [CrossRef]
45. Răcuciu, M.; Tecucianu, A.; Oancea, S. Impact of magnetite nanoparticles coated with aspartic acid on the growth, antioxidant enzymes activity and chlorophyll content of maize. *Antioxidants* **2022**, *11*, 1193. [CrossRef]
46. Behera, T.; Swain, P.; Rangacharulu, P.V.; Samanta, M. Nano-Fe as feed additive improves the hematological and immunological parameters of fish, *Labeo rohita* H. *Appl. Nanosci.* **2014**, *4*, 687–694. [CrossRef]
47. Ates, M.; Demir, V.; Arslan, Z.; Kaya, H.; Yılmaz, S.; Camas, M. Chronic exposure of tilapia (*Oreochromis niloticus*) to iron oxide nanoparticles: Effects of particle morphology on accumulation, elimination, hematology and immune responses. *Aquat. Toxicol.* **2016**, *177*, 22–32. [CrossRef]
48. Yin, Y.; Hu, B.; Yuan, X. Nanogel: A versatile nano-delivery system for biomedical applications. *Pharmaceutics* **2018**, *12*, 290. [CrossRef]
49. El-Naggar, M.E.; Radwan, E.K.; El-Wakeel, S.T.; Kafafy, H.; Gad-Allah, T.A.; El-Kalliny, A.S.; Shaheen, T.I. Synthesis, characterization and adsorption properties of microcrystalline cellulose based nanogel for dyes and heavy metals removal. *Int. J. Biol. Macromol.* **2018**, *113*, 248–258. [CrossRef]
50. Neamtu, I.; Rusu, A.G.; Diaconu, A.; Nita, L.E.; Chiriac, A.P. Basic concepts and recent advances in nanogels as carriers for medical applications. *Drug Deliv.* **2017**, *24*, 539–557. [CrossRef]

51. Hamdy, A.; Ismail, S.H.; Ebnalwaled, A.A.; Mohamed, G.G. Characterization of superparamagnetic/monodisperse PEG-coated magnetite nanoparticles sonochemically prepared from the hematite ore for Cd (II) removal from aqueous solutions. *J. Inorg. Organomet. Polym. Mater.* **2021**, *31*, 397–414. [CrossRef]
52. Hassan, G.K.; Abdel-Karim, A.; Al-Shemy, M.T.; Rojas, P.; Sanz, J.L.; Ismail, S.H.; Mohamed, G.G.; El-gohary, F.A.; Al-Sayed, A. Harnessing Cu@$Fe_3O_4$ core shell nanostructure for biogas production from sewage sludge: Experimental study and microbial community shift. *Renew. Energy* **2022**, *188*, 1059–1071. [CrossRef]
53. Košak, A.; Lobnik, A.; Bauman, M. Adsorption of mercury (II), lead (II), cadmium (II) and zinc (II) from aqueous solutions using mercapto-modified silica particles. *Int. J. Appl. Ceram.* **2015**, *12*, 461–472. [CrossRef]
54. Phippen, B.; Horvath, C.; Nordin, R.; Nagpal, N. *Ambient Water Quality Guidelines for Iron, Prepared for Science and Information Branch, Water Stewardship Division*; Ministry of Environment: Madrid, Spain, 2008; p. 45.
55. Kasozi, N.; Tandlich, R.; Fick, M.; Kaiser, H.; Wilhelmi, B. Iron supplementation and management in aquaponic systems: A review. *Aquac. Rep.* **2019**, *15*, 100221. [CrossRef]
56. Neiffer, D.L.; Stamper, M.A. Fish sedation, anesthesia, analgesia, and euthanasia: Considerations, methods, and types of drugs. *ILAR J.* **2009**, *50*, 343–360. [CrossRef]
57. Lee, Y.C.; Yang, D. Determination of lysozyme activities in a microplate format. *Anal. Biochem.* **2002**, *310*, 223. [CrossRef]
58. Abdollahi, R.; Heidari, B.; Aghamaali, M. Evaluation of lysozyme, complement C3, and total protein in different developmental stages of Caspian kutum (*Rutilus frisii kutum* K.). *Arch. Pol. Fish.* **2016**, *24*, 15–22. [CrossRef]
59. Bai, F.; Ni, B.; Liu, M.; Feng, Z.; Xiong, Q.; Xiao, S.; Shao, G. Mycoplasma hyopneumoniae-derived lipid-associated membrane proteins induce apoptosis in porcine alveolar macrophage via increasing nitric oxide production, oxidative stress, and caspase-3 activation. *Vet. Immunol. Immunopathol.* **2013**, *155*, 155–161. [CrossRef]
60. Schultz, L. *Methods in Clinical Chemistry*; CV Mosby Company: St. Louis, MO, USA, 1987; pp. 742–746.
61. Siroka, Z.; Krijt, J.; Randak, T.; Svobodova, Z.; Peskova, G.; Fuksa, J.; Hajslova, J.; Jarkovsky, J.; Janska, M. Organic pollutant contamination of river Elbe assessed by biochemical markers. *Acta Vet.* **2005**, *74*, 293–303. [CrossRef]
62. Ohkawa, H.; Ohishi, N.; Yagi, K. Assay for lipid peroxides in animal tissues by thiobarbituric acid reaction. *Anal. Biochem.* **1979**, *95*, 351–358. [CrossRef]
63. Beutler, E.; Duron, O.; Kelly, B.M. Improved method for the determination of blood glutathione. *J. Lab. Clin. Med.* **1963**, *61*, 882–888. Available online: https://pubmed.ncbi.nlm.nih.gov/13967893/ (accessed on 6 July 2023).
64. Velkova-Jordanoska, L.; Kostoski, G.; Jordanoska, B. Antioxidative enzymes in fish as biochemical indicators of aquatic pollution. *Bulg. J. Agric. Sci.* **2008**, *14*, 235–237.
65. Aksnes, A.; Njaa, L.R. Catalase, glutathione peroxidase and superoxide dismutase in different fish species. *Camp. Biochem. Physiol.* **1981**, *69B*, 893–896. [CrossRef]
66. Suvarna, K.S.; Layton, C.; Bancroft, J.D. *Bancroft's Theory and Practice of Histological Techniques E-Book*; Elsevier Health Sciences: Amsterdam, The Netherlands, 2018; p. 672.
67. Goldberg, E.D.; Koide, M.; Hodge, V.; Flegel, A.R.; Martin, J. US mussel watch: 1977–1978 results on trace metals and radionuclides. *Estuar. Coast. Shelf Sci.* **1993**, *16*, 69–93. [CrossRef]
68. Yacoub, A.M.; Gad, N.S. Accumulation of some heavy metals and biochemical alterations in muscles of *Oreochromis niloticus* from the River Nile in Upper Egypt. *Int. J. Environ. Sci. Eng.* **2012**, *3*, 1–10.
69. Kaplan, E.L.; Meier, P. Nonparametric-estimation from incomplete observations. *J. Am. Stat. Assoc.* **1958**, *53*, 457–481. [CrossRef]


**Disclaimer/Publisher's Note:** The statements, opinions and data contained in all publications are solely those of the individual author(s) and contributor(s) and not of MDPI and/or the editor(s). MDPI and/or the editor(s) disclaim responsibility for any injury to people or property resulting from any ideas, methods, instructions or products referred to in the content.